

## Liraglutide Nano-Preparation on Perioperative Neurocognitive Dysfunction in Aged Mice

Jiejie Zhang<sup>1,2#</sup>, Jie Song<sup>2#</sup>, Tianyu Gu<sup>2</sup>, Jiafeng Sun<sup>2</sup>, Xuejiao Cai<sup>2</sup>, Mengmeng Cai<sup>2</sup>, Jianping Yang<sup>1\*</sup>

<sup>1</sup>Department of Anesthesiology, The First Affiliated Hospital of Soochow University, Suzhou, 215006, China

<sup>2</sup>Department of Anesthesiology, The Second Affiliated Hospital of Nantong University, Nantong 226001, China

#These authors contributed equally to this work as co-first author

### ARTICLE INFO

#### Original paper

#### Article history:

Received: November 12, 2021

Accepted: March 12, 2022

Published: March 31, 2022

#### Keywords:

Liraglutide Nano-Preparation, perioperative neurocognitive dysfunction, Real Time PCR, Western Blot

### ABSTRACT

At present, there is not enough research about the application of liraglutide nano preparations in perioperative neurocognitive dysfunction. Therefore, the purpose of this study is the mechanism of the effect of liraglutide nano preparations on perioperative neurocognitive dysfunction in aged mice. In this study, 140 male SD rats aged 6-8 weeks were used as the research object, and were divided into 4 groups (n=24) according to the random number table method, which were group C (control group), group S (model group), and treatment. Group (low-dose liraglutide pretreated control group) and DS2 group (high-dose liraglutide pretreated control group) were treated with liraglutide anesthesia to establish a cognitive dysfunction model. Morris water maze experiment was conducted 4 days after anesthesia to compare the escape latency and the number of crossings of the original platform in each group; after 4 days of anesthesia, 18 old mice were randomly selected from each group for fluorescence quantitative polymerase chain reaction (Real Time PCR) and protein Western blotting (Western Blot) was used to determine the mRNA and protein levels of Caspase-3, Bax and Bcl-2 in the hippocampus; the remaining 6 old mice in each group were taken to observe the pathological changes of the hippocampus neurons by transmission electron microscopy. Compared with saline-treated group, the levels of NF- $\kappa$ B, TNF- $\alpha$  and IL-1 $\beta$  protein in mice treated with liraglutide decreased and I $\kappa$ B increased significantly (p<0.05). Liraglutide intervention may alleviate non-alcoholic fatty liver in diabetic mice by reducing the expression of inflammatory genes in liver tissue, thereby improving neurocognitive dysfunction in mice.

DOI: <http://dx.doi.org/10.14715/cmb/2022.68.3.39>

Copyright: © 2022 by the C.M.B. Association. All rights reserved



### Introduction

Cognitive dysfunction refers to the disorder or decline of the brain's advanced intelligent processing (1-2), such as thinking judgment, logical reasoning and problem solving (3-4), resulting in dysfunction of thinking, learning, memory and logical reasoning (5). According to the different degree and severity of cognitive impairment (6-7), the degree of cognitive impairment can be divided into three levels (8-9) from light to heavy: mild cognitive impairment, amnesia and dementia, which can be manifested as memory loss, psychomotor block, dementia, delirium, fine motor coordination difficulties and advanced cognitive impairment (10-11). Liraglutide is a biosynthetic GLP-1 analog (12-13) developed by danmeno and Nord pharmaceutical companies, and it is also a receptor agonist of GLP-1 (14). Its protein sequence is highly homologous with GLP-1 (15), and

only two amino acid positions are modified (16). Liraglutide can improve the survival rate of mice with neurocognitive impairment (17), and its function of remodeling myocardial cells is independent of hypoglycemic effect (18-19). For cognitive dysfunction, such as the choice of liraglutide nano preparation to promote the synthesis and transport of related neurotransmitters and other means to improve the symptoms of cognitive dysfunction (20-21), this study has great significance.

### Materials and Methods

The test object was 140 male SD old mice, 6-8 weeks old, weighing 260±20g, purchased from a laboratory animal technology company in Beijing. Animals are housed in SPF-level animal rooms. They can eat and drink water freely. The temperature of the feeding room is 22~24°C, the relative humidity is

\*Corresponding author. E-mail: [wulanmeng80455@163.com](mailto:wulanmeng80455@163.com)  
Cellular and Molecular Biology, 2022, 68(3): 356-364

about 50%, 12h light is 12h dark (light time 6:00-18:00), regular ventilation (22-23).

Experimental equipment includes freezer, ultrasonic tissue and cell disruption instrument, constant temperature oscillator, constant temperature water bath, high-speed low-temperature centrifuge, protein electrophoresis instrument, membrane transfer instrument, WD-9405 horizontal decolorization shaker, fluorescent gel imaging analysis system, Victor3 multi-functional microplate reader, tissue homogenizer, micro pipette, biological tissue embedding machine, paraffin slicer, electric thermostat, laser confocal fluorescence microscope, Image-pro plus 6.0 image analysis software, gene amplification instrument, Fluorescence quantitative PCR instrument, trace nucleic acid quantitative instrument, vertical electrophoresis instrument.

After three days of adaptive feeding of the purchased mice, the old mice were randomly divided into 4 groups: control group 20 (group C, intraperitoneal injection of equal volume of normal saline at the same time point); model group 40 (LPS100ug/Kg+S group, Intraperitoneal injection of LPS100ug/Kg+ left nephrectomy 1 hour before

surgery; 40 rats in the treatment group (L+LPS100ug/Kg+S group, intraperitoneal injection of liraglutide 10mg/Kg/d+ left nephrectomy for 3 consecutive days before surgery + Postoperative intraperitoneal injection of liraglutide 2mg/Kg/d until sacrifice); 40 rats in the liraglutide group (group L, intraperitoneal injection of the same amount of liraglutide nano preparations at the same time point); the model group was established with the same One part is divided into two groups. Among them, the first group (10 in each group, except Group C) was subjected to water maze test on the 3rd and 7th day after operation, and was killed according to relevant experimental requirements. Another group (10 animals in each group, except group C) performed conditional fear tests on the 3rd and 7th postoperative days, and were killed according to relevant experimental requirements. The water labyrinth test and the conditional fear test simultaneously conduct spontaneous activity tests (24-25). The experimental technology roadmap and the flow chart of the liraglutide nano-formulation administration experiment are shown in Figure 1.

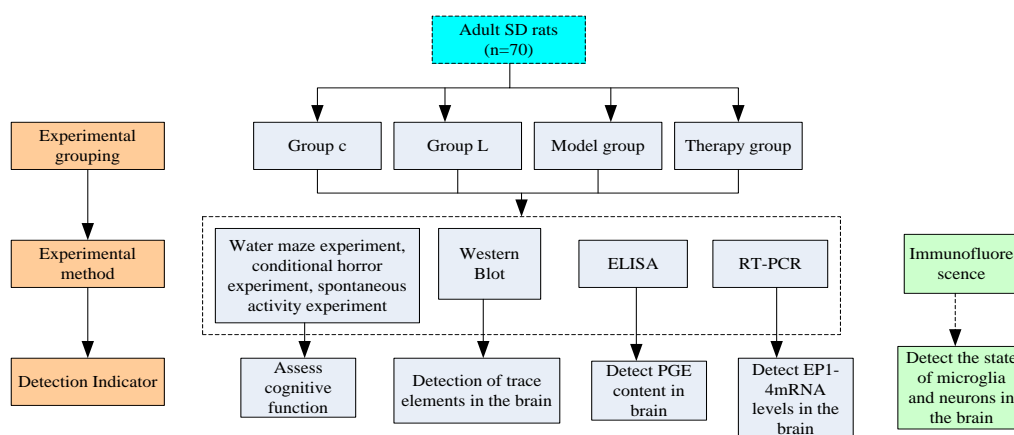


**Figure 1.** Experimental technology diagram based on liraglutide nano preparation

Use Excel tables to sort and correct the data, and use SPSS19.0 software for statistical analysis, including single-factor analysis using chi-square test, multi-factor analysis using unconditional logistic regression analysis, test level  $\alpha=0.05$ ,  $P \leq 0.05$ . The difference was statistically significant.

### Preparation of Liraglutide Nano Formulation

The steps were as follows:

{1} 30% Acr-Bis: Acrylamide (Acr) 29g, N-N' Methylenebisacrylamide (Bis) 1g, ultrapure water to 100ml, 4°C protected from light.

{2} 1.5M Tris-HCl (pH8.8): 18.165g Tris is dissolved in 80ml ultrapure water, after dissolving, adjust the pH value to 8.8 with 2.5M HCl solution, dilute to 100ml, and store at 4°C.

{3} 1 M Tris-Hcl (pH6.8): 12.1g Tris is dissolved in 80ml of ultrapure water. After dissolving, adjust the pH to 6.8 with HCl, dilute to 100ml, and store at 4°C.

{4} 10% SDS: SDS 10g, fully dissolved in 100ml ultrapure water, and stored at room temperature.

{5} 10% ammonium persulfate (AP): 0.1gAP, dissolved in 1ml ultrapure water, newly prepared before use.

{6} Electrophoresis buffer (5x stock solution): Tris 15.1g, glycine 94g, SDS 5g, ultrapure water 800ml, after the magnetic stirrer is fully dissolved, adjust the pH to 8.3, add ultrapure water to bring the volume to 1000ml, Store at 4°C. Take 100ml with ultrapure water and dilute 5 times when using.

{7} Transfer membrane buffer (10x stock solution): Tris 58g, glycine 29g, SDS 0.37g, ultrapure water 800ml, after the magnetic stirrer is fully dissolved, adjust the pH to 8.3, add ultrapure water to bring the volume to 1000ml, Store at 4°C. When using, take 50ml, add 50ml methanol, and add ultrapure water to 500ml.

{8} 5% skim milk powder blocking solution: 5g skim milk powder, add 1xTBS buffer solution to dissolve to 100ml, and store at 4°C.

{9} 5% BSA blocking solution: 5g BSA, add 1xTBS buffer solution to dissolve to 100ml, and store at 4°C.

{10} Anti-dilution solution: 5% skim milk diluted antibody Tau5, actin, GAPGH, R6ld, Akt, GSK-3B dilution ratio is 1:1000; 5% BSA diluted antibody Tau[pS396], Tau[pS214], Tau[pT205], Tau[pT212], Tau[pT231], Phospho-Akt (Ser473), Phospho-GSK3 $\beta$  (Ser9), Bcl-2, Bax, Caspase-3, secondary antibody dilution: 5% skim milk diluted horseradish Oxidase-labeled goat anti-mouse/rabbit IgG, dilution ratio 1:1000.

Step 1: Sample preparation: According to the protein concentration of each group of SH-SY5Y cells measured by the BCA method, add the corresponding volume of ultrapure water and buffer, adjust the final concentration of cell protein samples of each group to 2.5ug/ul, and mix well to the water bath Boil in the pot for 15 minutes to make Western blot buffer and store at 4°C. Boil and mix for 3 minutes before loading each sample.

Step 2: Preparation of mini electrophoresis gel: clean the glass plate, comb teeth, and glue maker, dry naturally, install the glue maker with 1.5mm glue sheet, keep the two plates flush, check the tightness of the glue distribution device to prevent leakage glue. According to the molecular weight of the target

protein, prepare a suitable concentration of separation gel (10%: Tau protein, Akt, GSK-3 $\beta$ ; 15%: Bcl-2, Bax, caspase-3, GAPDH; 7.5%: NFs), and seal with ultrapure water After air and glue solidify, pour off the ultrapure water on the surface, infuse 5% concentrated glue, and insert comb teeth.

Step 3: Sample addition: After the concentrated gel is solidified, pull out the comb teeth, put the concave surface of the glass plate in the electrophoresis tank, rinse the lanes with electrophoresis solution, use a pipette to draw the same amount of samples from each group into each lane, and add the pre-stained protein Marker2ul on the side lane. The sample load depends on the sensitivity of the antibody, about 30-60ug.

Step 4: SDS-PAGE electrophoresis: first electrophoresis with constant voltage 80V for about 30min. When the bromocool blue indicator is electrophoresed to the line between the concentration gel and the separation gel, change to constant voltage 100V electrophoresis for about 60min to bromophenol blue When separating the bottom of the gel, stop electrophoresis.

Step 5: Transfer membrane: transfer the protein from the SDS-PAGE gel to the PVDF membrane. Cut the PVDF membrane of the same size as the gel, soak it in formaldehyde, soak it in the membrane transfer solution with some of the same size filter paper, and follow the order of positive electrode (white) to negative electrode (black). Put the upper sponge, three layers of filter paper, PVDF membrane, gel, three layers of filter paper, sponge, layer by layer to remove air bubbles in sequence, buckle the transfer clip, put it in the transfer tank, make sure that the gel faces the negative electrode and the film faces positive electrode. Add cold transfer membrane buffer to the transfer tank, place the membrane transfer device in ice water, and turn on the electrophoresis instrument to adjust the constant current 300mA membrane transfer time according to the molecular weight of the target protein.

Step 6: Blocking: PVDF membrane is immersed in 5% skimmed milk powder or 5% BSA blocking solution, shaken slowly at room temperature for 30 min to block non-specific binding sites on PVDF membrane.

Step 7: Anti-incubation: seal the PVDF membrane in a plastic bag of suitable size, add the diluted primary antibody, remove the bubbles on the surface

of the PVDF membrane, seal the bag, and overnight at 4°C.

Step 8: Wash the membrane with 0.01M pH7.4 TBS or TBST (0.1% Tween20) for 5minx3 times.

Step 9: Secondary antibody incubation: PVDF membrane is incubated with diluted horseradish peroxidase-labeled goat anti-mouse or goat anti-rabbit IgG, and shaken slowly at room temperature for 90 minutes.

Step 10: Wash the membrane with 0.01M pH7.4TBS/TBST for 5minx3 times.

Step 11: ECL chemiluminescence color development: put the PVDF film in the exposure cassette, add the ECL (A liquid: B liquid = 1:1) mixed working droplets to the PVDF film, react in the dark room for 1min, wrap the plastic wrap In the cassette, cover the film on the upper layer of the PVDF film, close the exposure box, and the compression time depends on the antibody binding efficiency. After removing the film, rinse with developer, water, fixing solution, and water.

Step 12: Scan the film and analyze the band density with ImageJ software.

## **Preparation of Brain Neurocognitive Model**

### ***Cognitive Function Test-Morris Water Maze Experiment***

The Morris water maze judges the animal's learning and memory by observing the animal's behavior. It is used to study the evaluation of brain function related to spatial learning and memory. It is the first classic experiment for conducting behavioral research, especially learning and memory research. The Morris water maze is composed of a circular pool with a diameter of 120cm and a height of 50cm. It is divided into 4 quadrants, each quadrant is provided with a water point mark, and a rough surfaced transparent platform with a diameter of 6cm and a height of 30cm is set in the third quadrant. The water depth in the pool is 25cm, the water temperature is controlled at 21~22°C, and an automatic camera system is installed above the pool. The water labyrinth experiment includes the directional navigation experiment and the space exploration experiment, which were conducted for 5 days. (1) Directional navigation experiment: for 4 days, it mainly detects the ability of mice to obtain spatial information. Training 4 times a day, from 9:00-11:00 in the morning, put the mice into the water

from the four quadrants into the water wall, record the time to find the platform (escape latency) within 60 seconds, and let the mouse in Stay on the platform for 10 seconds. Those who failed to find the platform or climbed to the platform after more than 60 seconds, gently guided it to the platform with a wooden stick and stayed for 10 seconds, setting the time for finding the platform to 60 seconds. Take the average value of the measurement results of each mouse 4 times as the escape latency of the mouse that day, and record the swimming speed of each mouse. The shorter the time required to find the platform, the better the ability to obtain spatial information. (2) Space exploration experiment: for a period of 1d, it mainly evaluates the ability of mice to remember the spatial location of the platform. After 24 hours of the directional navigation test, the platform was dropped, and the mouse was placed into the water facing the tank wall at the same water inlet point. The swimming path of the mouse in 60 seconds was recorded, the number of crossings of the mouse on the original platform and the third quadrant activity were recorded. time. Record related data and image results through Morris water maze data collection and analysis software.

### ***Sd Mouse Was Established with Reference to the Modified Longa Thread Suppository Method to Establish a Neurocognitive Model of the Brain***

Specific steps:(1) Fasting for 12 hours before operation and weighing.(2) 10% chloral hydrate is anesthetized by intraperitoneal injection at 30-35mg/kg kg body weight.(3) After the anesthesia is successful (muscle relaxation, corneal reflex disappearance, pain and irritation does not respond), fix the mouse in the supine position on the operating table. Prepare the skin for disinfection, cut the skin along the middle of the neck, and the subcutaneous tissue is blunt Separation, separating the right common carotid artery, external carotid artery, internal carotid artery, ligating the proximal end of the common carotid artery and the distal end of the external carotid artery, the arterial vascular clip clips the distal end of the internal carotid artery, and the proximal end is divided Leave a line at the fork to spare. Cut a small slit in the common carotid artery and insert a nylon thread plug. When the thread plug enters the internal carotid artery, remove the vascular clamp and slowly insert it. When the distance from the

common bifurcation of the neck is  $18\pm 0.5$ mm (just feel the resistance), tighten it for use Wire fixing wire bolt. Suture skin incision and disinfect. Keep warm after surgery.

### **Neurological Score**

The neurological function score of SD male aging mice is mainly based on the score scale of the percentage system: 0 points: normal, without symptoms of neurological deficit; 20 points: the contralateral front paw cannot be fully extended; 40 points: the resistance decreases when applying force to the opposite side of the operation; 60 points: turning to the opposite side of the operation when walking; 80 points: Pour to the opposite side of the operation when walking; One hundred points: Can't walk and lose consciousness, no response to pain stimuli. Mice in each group were scored for neurological deficit 24 hours after cerebral ischemia. Mice with scores of 0, 100, and dead were excluded, and randomly remodeled. The old mice in each group were scored and recorded for analysis.

### **Staining to Measure Cerebral Infarction Volume**

The volume of cerebral infarction was measured by 2,3,5-chlorine 0 staining method with no recognition result. Six animals from each group were randomly selected and scored for neurological deficit at 24h of cerebral ischemia. After decapitation, the brain was removed by anesthesia (taken on ice) and immediately placed in a refrigerator at  $-20^{\circ}\text{C}$  for about 10 minutes and cut along the coronal position. 5 pieces, about 2mm thick. Place in 2% TTC buffer, incubate at  $37^{\circ}\text{C}$  in tin foil paper in the dark for 30 min, remove the brain slice and fix it with 4% paraformaldehyde for 24 h, then take a picture, and use the ImageJ software to determine the volume of cerebral infarction.

### **Superoxide Dismutase (SOD) and Myeloperoxidase (MPO) Activity Detection**

The remaining 6 old mice in each group were decapitated and the brains were collected. The brain tissue was stored in a refrigerator at  $-80^{\circ}\text{C}$  and taken at any time. Take brain tissue of the same quality, add 4% 0.9% NaCl at 1:9, homogenize to make 10% tissue fluid, centrifuge (4000 rpm, 10min), and then take the supernatant. Follow the instructions of SOD and MPO kits.

### **Organizing Specimen Collection and Processing**

After the cognitive function test was completed, 6 mice from each group were taken off the neck and sacrificed. The chest cavity was opened and the venous cannula was inserted from the left ventricle to the ascending aorta. The right atrial appendage was cut, and about 300 ml of  $4^{\circ}\text{C}$  normal saline was quickly infused. When the outflow of blood became clear, replace with about 500 ml of formalin solution, and then perfuse and fix it for about 20 minutes, then separate the intact brain tissue on the ice. After the brain was taken out and put into formalin solution for fixation overnight, it was dehydrated by gradient alcohol, xylene was transparent, and low-melting paraffin was embedded. Paraffin block is oriented sliced, thickness is 4um, placed on polylysine-coated glass slide, baked in a  $56^{\circ}\text{C}$  incubator for 2h, stored at room temperature, used for HE staining, Nessler staining and immunofluorescence staining. After the remaining mice in each group were taken off the neck and sacrificed, the hippocampus was quickly taken out on the ice. Part of the hippocampus was stored at  $-80^{\circ}\text{C}$ , which was used for Western blotting and Real-time RT-PCR detection. Aldehyde fixation, used for transmission electron microscopy.

### **Basic Properties of Liraglutide**

Liraglutide can resist AD-like neurodegeneration induced by  $\text{H}_2\text{O}_2$ , and its mechanism may improve cell survival, inhibit apoptosis, and improve abnormal phosphorylation of Tau protein and NFs in nerve cells by activating PI3K-Akt signaling pathway. Play a neuroprotective role. On this basis, liraglutide can also lower blood sugar and improve insulin resistance, as well as reduce body weight, body mass index, diastolic blood pressure and triglycerides, total cholesterol, low-density lipoprotein index levels, which may indirectly delay neurocognitive function Obstacles to development.

### **Determination of Apoptosis in Neurocognitive Function**

{1} The human umbilical vein endothelial cells with different treatments were fixed in 10% formaldehyde solution for two days, followed by multi-step dehydration and paraffin embedding treatment. The processed wax block is continuously

sliced under a microtome, and the thickness of each piece is 2 $\mu$ m.

{2} The slices were gradually dehydrated with gradient ethanol, and then rinsed with PBS solution 3 times, at least 5 minutes each time.

{3} Use 20  $\mu$ g/mL proteinase K solution to digest at 37 degrees for 15 minutes, then rinse with distilled water 3 times, at least 5 minutes each time.

{4} Preheat the slices in an oven with a temperature of 60 degrees, take them out at room temperature for 40 minutes, soak them in 3% hydrogen peroxide for 15 minutes, and then rinse them with PBS solution 3 times for at least 5 minutes each time.

{5} Wipe the slice clean with absorbent paper, add 50 $\mu$ L of the labeled reaction solution in the middle of the slice, place it in a 37-degree wet box, and then rinse with PBS solution 3 times for at least 3 minutes each time.

{6} 50 $\mu$ L POD was added dropwise in the middle of the slice, placed in a 37 degree wet box for half an hour, and then rinsed with PBS solution 3 times, at least 5 minutes each time.

{7} Add 100 $\mu$ L DAB dye solution for color development, and observe the color development of the section under the microscope.

{8} Counterstain with hematoxylin for two minutes, add ammonia to quickly turn blue.

{9} Observe the slice result under the microscope after dehydration, transparency and drying.

{10} Calculate the apoptotic index of umbilical vein endothelial cells: select three different fields of view under a microscope of 400 times, and count the total number of umbilical vein endothelial cells and the number of apoptotic cells, of which the nucleus of apoptotic cells is brownish yellow, Normal cells are stained blue. Apoptosis index (AI) = (apoptotic umbilical vein endothelial cells/total umbilical vein endothelial cells) \* 100%.

## Results and Discussion

### Behavioral Examination after Injecting Liraglutide into The Brain of Aged Mice

Twelve weeks after injecting liraglutide, we used the Morris water maze to test the cognitive function of aging mice in each group. In the directional navigation experiment, the incubation period from the time when the mouse entered the water to find the hidden escape platform was selected as the evaluation

index. The results showed that the incubation period of the old mice in the simple irradiation group (R group) during the 5 days of the directional navigation experiment was significantly longer than that of the control group (C group). After injecting liraglutide, compared with the R group, the incubation period of mice in the R+GFP-NSCs group and R+GFP-BDNF-NSCs group to find the hidden platform was not significantly shortened. The specific image is shown in Figure 2. In the space exploration experiment, the R group, R+GFP-NSCs group and R+GFP-BDNF-NSCs group mice stayed in the target quadrant as a percentage of the total time was significantly lower than the control group, as shown in Figure 3. These results indicated that aged mice showed significant cognitive dysfunction after 16 weeks of 20Gy whole brain irradiation, but the transplantation of GFP-NSCs and GFP-BDNF-NSCs failed to effectively improve the cognitive function of aged mice exposed to radiation.

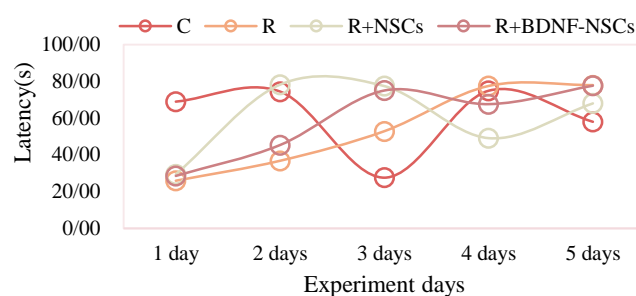


**Figure 2.** Comparison of 4 groups of experiments after 5 days of old mice

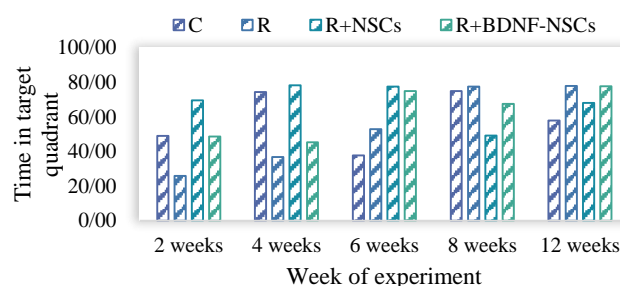


**Figure 3.** Comparison of 4 groups of experiments after 12 weeks of old mice

### Effect of Liraglutide on Learning and Memory Abilities of Aged Mice

The positioning navigation experiment was carried out for 4 consecutive days, and each old mouse was subjected to four rounds of experiments every day.

Each round of experiments put the mice into the water from the water inlet points of the four quadrants to the wall of the pool. Each round of the experiment was conducted for 90s, and the old mice were recorded. The time to find the platform (escaping incubation period). If the platform is not found within 90s of the old mouse, the experimenter should guide the mouse to the platform and let it stay for 10s. The escape incubation period of the mouse is recorded as 90s. Record the time to find the platform and the swimming trajectory of the old mice in 4 rounds of experiments. The longer the incubation period, the worse the learning ability of the mice. The specific experimental data is shown in Table 1, the specific analysis image of the escape latency is shown in Figure 4, and the specific analysis image of the total swimming distance is shown in Figure 5.

**Table 1.** Results of the positioning navigation experiment of the old mice in each group

Group	Escape latency (s)	Total swimming distance (cm)
Blank control group	21.99±3.21	898.2±45.81
Model group	31.75±5.21	1101.5±114.85
Positive drug group	35.26±7.72	987.5±63.22
Liraglutide low-dose group	52.51±3.58	856.2±56.47
Liraglutide mid-dose group	55.84±5.48	998.3±43.63
Liraglutide high-dose group	56.49±5.38	902.5±36.74

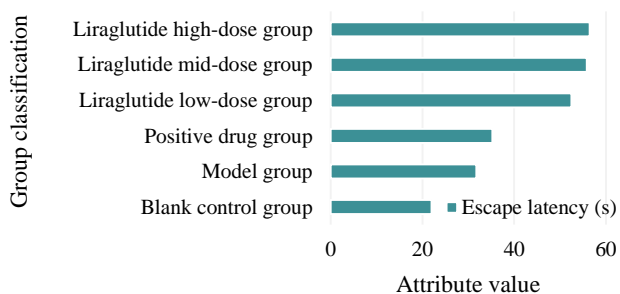


**Figure 4.** The escape latency of each group after 4 days of experiment

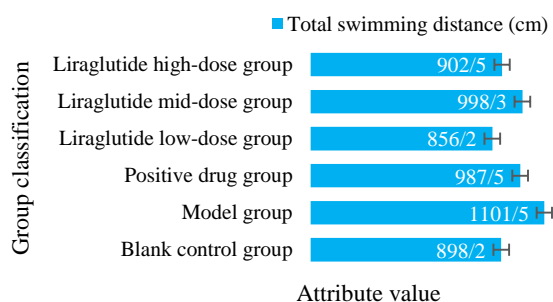


**Figure 5.** The total swimming distance of each group after 4 days of experiment

Compared with the blank group, the mice in the model group found that the escape latency was significantly prolonged ( $P < 0.01$ ), and the total swimming distance was significantly increased ( $P < 0.01$ ); compared with the model group, the mice in the positive drug, liraglutide, and high-dose groups escaped. The incubation period was shortened ( $P < 0.05$ ), and the total swimming distance was reduced ( $P < 0.05$ ,  $P < 0.01$ ).

**Changes in Mice and Body Weight and Serum TG, CHO, LDL**

By testing the blood biochemical indexes of the three groups of model mice, we can see that the weight of the model group mice, the level of triglycerides in the blood, the level of total cholesterol and the value of LDL are the highest, which is statistically compared with the blank group Significance ( $P < 0.05$ ). In contrast, although the weight of the old mice in the liraglutide group, the level of triglyceride in the blood, the level of total cholesterol and the value of LDL were also higher than the blank group, but compared with the model group, it was reduced, It is statistically significant ( $P < 0.05$ ), as shown in Table 2.

**Table 2.** Changes of TG, CHO and LDL in the body and serum of aged mice

Index	Blank group(n=15)	Model group(n=15)	Liraglutide group(n=15)	F value	P value
Weight (g)	7.12±43.82	761.14±82.11	743.24±71.35	41.242	<0.002
TG(mmol/L)	3.79±0.36	1.39±0.24	1.21±0.314	24.934	<0.002
CHO(mmoVL)	6.54±0.84	2.16±0.43*	1.63±0.38	15.345	<0.002
LDL(mmoVL)	5.52±0.36	1.28±0.23*	0.78±0.264	54.575	<0.002

**Conclusions**

In this study, for the first time after adding liraglutide whole brain irradiation to aged mice with cognitive dysfunction, changes in dendritic spine density and morphology in different brain regions of the hippocampus over time, dendritic spine density and morphology were detected. The changes may be related to the decreased expression of synaptic-related proteins after ionizing radiation, which provides a morphological basis for the study of the pathogenesis of radiological cognitive dysfunction. In different grouping states, the hippocampus and prefrontal cortex of mice have different powers. First, under the non-task baseline state, the power spectrum of the prefrontal cortex and hippocampus found that there

was a difference in physiological characteristics between the prefrontal cortex and hippocampus before and after modeling. Second, the intra-group comparisons of mice before and after modeling were performed, and the power spectra of normal mice in the spatial and non-spatial memory stages and mice in the spatial and non-spatial memory stages were calculated, respectively, and the spatial and non-spatial task states were found. The power spectrum of the old mouse hippocampus in a specific frequency band is significantly increased, and the mouse is significantly reduced; that is, the spatial and non-spatial mission states of the old mouse hippocampus and prefrontal cortex Theta and Gamma rhythm power spectrum are significantly increased compared with the non-mission state. ; But after cognitive state, showed a corresponding decrease. Third, the old mice before and after modeling were compared between groups, and the results showed that the hippocampus was mainly involved in space tasks, and the prefrontal cortex was mainly involved in non-space tasks; that is, compared with no entry, the old mice under the space task, hippocampus The power spectrum of the Delta, Theta, and Gamma bands of the Delta, Theta, and Gamma bands of the prefrontal cortex decreased significantly.

### Acknowledgments

The research is supported by: Jiejie Zhang, Clinical Basic Research of Nantong University, (No. 2019JY006).

### Interest conflict

The authors declare that they have no conflict of interest.

### References

- Mann JF, Ørsted DD, Brown-Frandsen K, Marso SP, Poulter NR, Rasmussen S, Tornøe K, Zinman B, Buse JB. Liraglutide and renal outcomes in type 2 diabetes. *N Engl J Med* 2017;377(9):839-48.
- Cegla J. Liraglutide safety and efficacy in patients with non-alcoholic steatohepatitis (LEAN): a multicentre, double-blind, randomized, placebo-controlled phase 2 study. *Ann Clin Biochem* 2016;53(4):518-.
- Vedtofte L, Knop FK, Vilsbø L, T. Efficacy and safety of fixed-ratio combination of insulin degludec and liraglutide (IDegLira) for the treatment of type 2 diabetes. *Expert Opin Drug Saf* 2017;16(3):387-396.
- Farr OM, Sofopoulos M, Tsoukas MA, Dincer F, Thakkar B, Sahin-Efe A, Filippaios A, Bowers J, Srnka A, Gavrieli A, Ko BJ. GLP-1 receptors exist in the parietal cortex, hypothalamus and medulla of human brains and the GLP-1 analogue liraglutide alters brain activity related to highly desirable food cues in individuals with diabetes: a crossover, randomised, placebo-controlled trial. *Diabetologia*. 2016;59(5):954-65.
- Iacobellis G, Mohseni M, Bianco SD, Banga PK. Liraglutide causes large and rapid epicardial fat reduction. *Obesity* 2017;25(2):311-6.
- Ostawal A, Mocevic E, Kragh N, Xu W. Clinical effectiveness of liraglutide in type 2 diabetes treatment in the real-world setting: a systematic literature review. *Diabete Ther* 2016;7(3):411-38.
- Nozue T, Yamada M, Tsunoda T, Katoh H, Ito S, Iwaki T, Michishita I. Effects of liraglutide, a glucagon-like peptide-1 analog, on left ventricular remodeling assessed by cardiac magnetic resonance imaging in patients with acute myocardial infarction undergoing primary percutaneous coronary intervention. *Heart vessels*. 2016;31(8):1239-46.
- De Wit HM, Vervoort GM, Jansen HJ, De Galan BE, Tack CJ. Durable efficacy of liraglutide in patients with type 2 diabetes and pronounced insulin-associated weight gain: 52-week results from the Effect of Liraglutide on insulin-associated weight gain in patients with Type 2 diabetes (ELEGANT) randomized controlled trial. *J Intern Med* 2016;279(3):283-92.
- Tonneijck L, Smits MM, Muskiet MH, Hoekstra T, Kramer MH, Danser AJ, Ter Wee PM, Diamant M, Joles JA, Van Raalte DH. Renal effects of DPP-4 inhibitor sitagliptin or GLP-1 receptor agonist liraglutide in overweight patients with type 2 diabetes: a 12-week, randomized, double-blind, placebo-controlled trial. *Diabetes Care* 2016;39(11):2042-50.
- Barreto-Vianna AR, Aguila MB, Mandarim-de-Lacerda CA. Effects of liraglutide in hypothalamic arcuate nucleus of obese mice. *Obesity*. 2016;24(3):626-33.
- Gough SC, Jain R, Woo VC. Insulin degludec/liraglutide (IDegLira) for the treatment of type 2 diabetes. *Expert Rev Endocrinol Metab* 2016;11(1):7-19.
- Hu SY, Zhang Y, Zhu PJ, Zhou H, Chen YD. Liraglutide directly protects cardiomyocytes against reperfusion injury possibly via modulation of intracellular calcium homeostasis. *J Geriatr Cardiol* 2017;14(1):57.
- Kaku K, Kiyosue A, Ono Y, Shiraiwa T, Kaneko S, Nishijima K, Bosch-Traberg H, Seino Y. Liraglutide is effective and well tolerated in combination with an oral antidiabetic drug in Japanese patients with type 2 diabetes: a randomized, 52-week, open-label, parallel-group trial. *J Diabetes Investig* 2016;7(1):76-84.
- Kuhadiya ND, Dhindsa S, Ghanim H, Mehta A, Makdissi A, Batra M, Sandhu S, Hejna J, Green K, Bellini N, Yang M. Addition of liraglutide to insulin in patients with type 1 diabetes: a randomized placebo-

- controlled clinical trial of 12 weeks. *Diabetes Care*. 2016;39(6):1027-35.
15. de Vroege L, Timmermans A, Kop WJ, van der Feltz-Cornelis CM. Neurocognitive dysfunctioning and the impact of comorbid depression and anxiety in patients with somatic symptom and related disorders: a cross-sectional clinical study. *Psychol Med* 2018;48(11):1803-13.
  16. Chang Gu Kang, Min Ho Chun, Jung-A Kang. Neurocognitive Dysfunction According to Hypoperfusion Territory in Patients with Moyamoya Disease. *Ann Rehabil Med* 2017;41(1):1-8.
  17. Ellero J, Lubomski M, Brew B. Interventions for neurocognitive dysfunction. *Curr HIV/AIDS Rep* 2017;14(1):8-16.
  18. Bickel WK, Moody LN, Eddy CR, Franck CT. Neurocognitive dysfunction in addiction: Testing hypotheses of diffuse versus selective phenotypic dysfunction with a classification-based approach. *Exp Clin Psychopharmacol* 2017;25(4):322.
  19. Ahmed T, Karim MR, Khan JH, Moinuddin S. Evaluation of neurocognitive dysfunction after coronary artery bypass surgery. *Cardiovascular J* 2018;10(2):186-93.
  20. Hara S, Hori M, Murata S, Ueda R, Tanaka Y, Inaji M, Maehara T, Aoki S, Nariai T. Microstructural damage in normal-appearing brain parenchyma and neurocognitive dysfunction in adult moyamoya disease. *Stroke*. 2018;49(10):2504-7.
  21. M. Plohmann A, Hurter M. Prevalence of poor effort and malingered neurocognitive dysfunction in litigating patients in Switzerland. *Zeitschrift für Neuropsychologie* 2017;27(2):97-116.
  22. De Felice F, Blanchard P. Radiation-induced neurocognitive dysfunction in head and neck cancer patients. *Tumori J* 2017;103(4):319-24.
  23. van Kessel E, Baumfalk AE, van Zandvoort MJ, Robe PA, Snijders TJ. Tumor-related neurocognitive dysfunction in patients with diffuse glioma: a systematic review of neurocognitive functioning prior to anti-tumor treatment. *J neuro-oncol* 2017;134(1):9-18.
  24. Sha Z, Wager TD, Mechelli A, He Y. Common dysfunction of large-scale neurocognitive networks across psychiatric disorders. *Biol Psychiatry* 2019;85(5):379-88.
  25. Cichowitz C, Carroll PC, Strouse JJ, Haywood Jr C, Lanzkron S. Utility of the Montreal Cognitive Assessment as a screening test for neurocognitive dysfunction in adults with sickle cell disease. *South Med J* 2016;109(9):560.